ANALYTICAL CONTROL OF NICKEL COATING BATHS BY DIGITAL IMAGE ANALYSIS

Gorka Albizu, Ane Bordagaray, Sergio Dávila, Rosa Garcia-Arrona, Miren Ostra, and Maider Vidal

Department of Applied Chemistry, Faculty of Chemistry, University of Basque Country (EHU/UPV), 20080 San Sebastian, Spain

Keywords: Digital Image Analysis, nickel bath, sulfate, ammonium

Corresponding author: ane.bordagaray@ehu.eus

Abstract

Nickel plating is a widely employed technique. To carry out this, nickel baths are used, which require a great control of the concentration of its components. In this work, fast and cheap methods based on digital image analysis (DIA) are proposed to determine some of the major compounds in these baths such as nickel, ammonium and sulfate ions. The greatest advantage of these methods is the possibility of analyzing several samples at the same time using very small volumes, lower than 400 μL.

Simple and widespread equipment as a desktop scanner has been used to obtain the digital images. Using these images, linear regression models were built for each analyte, obtaining correlation coefficients higher than 0.99, RSD values lower than 14.0% and recoveries between 82 and 111% in all cases. The reproducibility of the images has been confirmed by a color standard. These methods have been applied successfully in real samples. The results obtained have been compared with reference techniques, such as UV-Vis spectrophotometry, ion chromatography and potentiometry. No significant differences were observed between these methods and the proposed digital image analysis method.

1. Introduction

Nickel is one of the most employed metals in the coatings industry. This is due to its high resistance to corrosion and abrasion, ferromagnetic properties and esthetic properties of the obtained coatings [1]. For this reasons, nickel plating is widely used in various sectors, such as computing, electronics, automotive…[2] Each year, 150.000 tons of nickel coating are deposited worldwide [3].

Nickel-plating process is carried out by nickel deposition baths. Depending on how Ni (II) is reduced to Ni^0, baths could be electroless or electrolytic baths. In both cases, it is important to control the physicochemical parameters, such as temperature, pH and stirring, in order to achieve coatings with the desired properties. Nevertheless, it is also essential to control the concentration of the different components of the bath formulation along the coating process.

Nickel sources usually are nickel sulfate salts, consequently nickel and sulfate are the compounds found in higher concentrations in the baths. To know the concentration of nickel, techniques such as atomic spectroscopy have been used [3,4,5]. However, due to the simplicity of the method and to the characteristic green color of nickel solutions, ultraviolet-visible spectrophotometric determination is the fastest option, measuring the absorbance at 394 nm [6,7]. On the other hand, ion chromatography has been used to determine sulfate, since chromatography allows several anions to be determined at the same time.[8]

Another compound present in many electroless nickel bath formulations is the ammonium ion. It has a complex function, preventing the sudden decomposition of the bath. In addition, it is added as pH control element. One of the most widespread methods for its determination is ion chromatography [9]. Nessler reagent can also be used, being able to quantify the ammonium by colorimetry (405 nm), obtaining a yellow-orange color [10].

In this work digital image analysis (DIA) has been the used for the determination of some ions in nickel baths, such as nickel, sulfate and ammonium. Image analysis is a set of

techniques focused on obtaining data from images [11]. Nowadays, DIA has gained increased interest for analytical chemistry applications due its simplicity, low-cost, speed and straightforward performance, compared with other instruments in the laboratory. Moreover, there is no need of large amount of sample; therefore, it is more respectful with the environment. Many works can be found in the literature in which image analysis has been used as an analytical technique for the classification of pesto sauces [12], determine color additives in food [13,14], or cyanides in water on paper basis [15], among others. This technique has also been used in the coating industry. For example, the prediction of surface roughness and crystallographic texture from scanned imaged of chromium electrodeposits has been proposed [16]. In the electrodeposition of nickel in particular, image analysis has been used to control the concentration of polishing additives by analyzing the brightness of the coating of steel sheets and to evaluate de quality of the deposition [17,18].

In many of the cases described in the literature, a desktop scanner has been used as image-taking device, but mobile phones or digital cameras can also be used. Image acquisition is the first step of the process, in which the device used and the illumination control play a fundamental role [19].

Once the image is taken, it can be converted into numerical values dividing the image in two-dimensional grids (pixels). The value of each pixel is described by color spaces, which can be composed of several channels. The most commonly used color space is the RGB, which can be decomposed into three primary colors: red, green and blue. Each of these colors or channels reaches values from 0 to 255, and the combination of these defines the final color of the pixels. Software packages like MATLAB allow applying algorithms to convert variables from one color space, like RGB, to another. Some of these color spaces are: Lab (or CIELab), adopted by the Commission International d'Eclairage (CIE) in 1976 where L represents lightness, and a and b mark the variations from red to green and yellow to blue; HSV (Hue, Saturation, Value)

a cylindrical-coordinate system in accordance with the feel of human eye and CMYK (cyan, magenta, yellow, key), which is used usually in color printing. [12] In this work, in addition to the RGB space, the HSV space has been used.

Finally, from the extracted information, a parameter that can be related to the analyte must be found. In some cases, this relationship is qualitative and allows classifying the analyzed samples, and in others, it is quantitative and allows determining analyte concentration.

The aim of this work was to develop and validate a digital image analysis control method for the quantification of the majority compounds of an electrolytic and electroless nickel baths, in this case nickel, ammonium and sulfate.

2. Experimental

2.1.Reagents and solutions

All chemical were of analytical reagent grade (Panreac, Aldrich or Probus) and doubly distilled water was used throughout. To prepare nickel and sulfate calibrations, pure $NiSO_4 \cdot 6H_2O$ (CAS number 10101-97-0) was employed. For the study of nickel, a stock solution containing 10 g L^{-1} Ni was prepared. In the case of sulfate, a stock of 1 g L^{-1} of SO_4^{2-} was used. Lower concentration solutions were prepared by appropriate dilution with doubly distilled water. A solution containing 10 g L^{-1} of $BaCl_2$, prepared from pure $BaCl_2 2H_2O$ (CAS number 10326-27-9), and 1.6 g L^{-1} of povidone (CAS number 9003-39-8) were prepared for sulfate determination. Besides, 1:10 dilution of HCl 37% was used. For ammonium determination, analytical grade NH_4Cl (CAS number 12125-02-9) was employed as standard. Nessler´s reagent was prepared from KI (CAS number 7681-11-0), Hg_2Cl (CAS number 7487-94-7) and NaOH (5M) (CAS number 1310-73-2).

The mobile phase solution used for ion chromatography was prepared from Na_2CO_3 $1.8 \cdot 10^{-3}$M (CAS number 497-19-8) and $NaHCO_3$ (CAS number 144-55-8) ($1.7 \cdot 10^{-3}$M). Finally, as a

stabilizer of the ionic strength for the potentiometric method, $MgSO_4$ (1M) (CAS number 10034-99-8) solution was used.

2.2.Employed samples

A total of 13 nickel bath samples were employed, 10 samples from a electroless nickel bath provided by CIDETEC Surface Engineering (Donostia, Spain) and three samples from an electrolytic nickel bath prepared in the laboratory according to the conditions described by M. Vidal *et al*.[20]

2.3.Apparatus and software

A desktop scanner Epson Stylus DX7400 was used as image-taking device, executed by Epson Scan software. For image treatment, the employed computer was a DELL Optiplex 7010 Intel® CORE™ i7 de 465GB, which has the MATLAB R2016b (The Mathworks, Inc. Natick, MA) software with the Image Processing Toolbox™ (The MathWorks, Natick, MA, USA).

Absorbance measurements were carried out with an Agilent 8453 UV-Visible spectrophotometer and the HP UV-Vis Win System software.

For ion chromatography, an 883 Basic IC plus Metrohm chromatograph coupled to a conductivity detector was used. The employed column was an anionic polyvinyl alcohol with quaternary ammonium groups covered with PEEK (250 mm x 4 mm). The software MagIC Net 3.2 was used for data acquisition and processing. Before measurements, standards and samples were filtered with a 0.45 μm nylon filters.

Finally, a pH-meter Crison GLP 22 (Barcelona, Spain) was used, with an ammonium selective electrode and lithium acetate electrode as a reference (Crison).

2.4.Analyte determination methods

For image acquisition, microtitration plates of 96 wells with a capacity of 400 μL were used. For nickel determination, dilutions were made from the stock solution with distilled water to

obtain concentrations in the range of 1 - 10 g L^{-1}. Due to the characteristic green color of nickel solutions, the concentration of the metal can be directly related to the obtained color.

In the case of sulfate, all reagents were mixed in wells obtaining concentration between 0.1 and 0.7 g L^{-1} of SO_4^{2-}. To obtain the white $BaSO_4$ precipitate, 10 µL of HCl, 100 µL of $BaCl_2$ and the required volume of SO_4^{2-} stock solution were added. Finally, doubly distilled water was added to complete a total volume of 400 µL. In all cases, the last added reagent was $BaCl_2$, in order to make the precipitation-reaction start at the same time in all wells. The image was taken 10 minutes after adding $BaCl_2$.

Finally, ammonium determination was carried out using the Nessler reagent. In this case, the reaction was prepared in 50 mL flasks and then 400 µL were transferred to the wells. Firstly, 2 mL of NaOH solution and another 2 mL of Nessler reagent were added to the flasks. The required volume of ammonium stock to obtain concentrations in the range of $1 \cdot 10^{-3}$–$5.0 \cdot 10^{-3}$ g L^{-1} was added before filling up the flask. Solutions turn to orange in presence of ammonium due to the following reaction:

$$2\,[HgI_4]^{2-} + 4\,OH^- + NH_4^+ \rightleftharpoons HgI(H_2N) \cdot HgO + 7\,I^- + 3\,H_2O$$

For DIA of all analytes, each solution was prepared in triplicate in the wells and then the average value of the chosen color channel was obtained. In addition, in all microtitration plates, three wells were filled with distilled water as a blank (Fig. 1.a).

(a) (b)

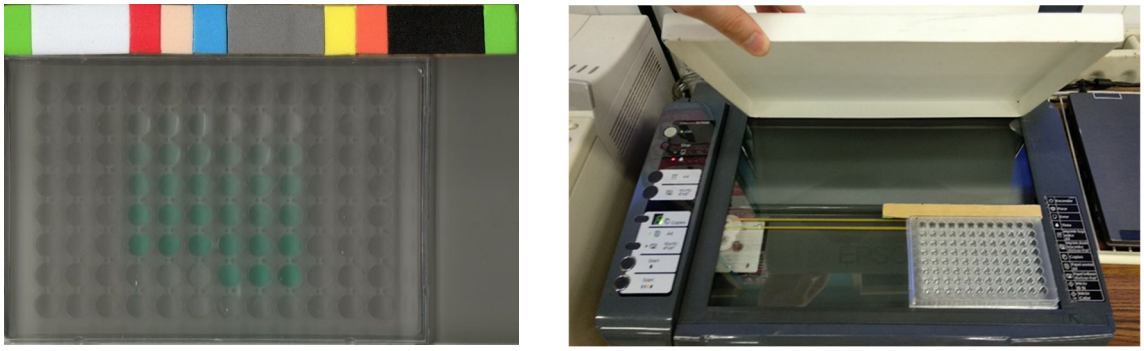

Figure 1. (a) Image of several nickel standards in the microtitration plate with 96 wells and the color standard (in the upper part of the image) used in each image to control the illumination conditions. (b) Image showing the used

system to acquire the digital images. An empty microtitration plate has been placed in the scanner window together with the color standard. The fabricated matte white cover is also shown.

2.5.Image acquisition and processing

Once the wells were filled and the color obtained, the image was taken. For that, the plate was placed on the scanner together with a color standard (Fig. 1.a). This type of standard, composed by 10 patches of different color, has been previously used as a control of the illumination and the reproducibility of images in the works by M. Vidal *et al.*[14,16,17,18]. The scanner offers certain advantages in comparison with smartphones and digital cameras in terms of lighting control, since the picture is taken in a close environment. In this case, a cover made of galvanized iron and painted in matt white with the same dimensions of the scanner window was made in order to avoid ambient light to affect the image measurements, as it is described in the work of M. Vidal *et al.*[14] (Fig. 1.b). This way, the scanner image acquisition conditions were controlled and the reproducibility of images ensured.

After uploading the images to the MATLAB software, the colored area of each well was cut in 11 x 11 pixel squares, employing a function designed specifically for it. From the cuts, the mean values of the R,G and B color channels were obtained in order to build univariate regression models..

2.6.Application to real samples

The employed samples can be divided into two groups: samples from an electroless nickel bath and from an electrolytic nickel bath. First ones are blue colored, due to the presence of ammonia, which forms a blue complex with nickel. Therefore, samples were acidified with diluted HCl directly in the wells, releasing the nickel and recovering the characteristic green color. In these acidified samples nickel, sulfate and ammonium were determined. On the other hand, in electrolytic bath samples only nickel and sulfate were determined. In both type of samples, recovery studies were also carried out at two levels of concentration for each analyte.

As reference methods, UV-Vis spectrophotometry, ion chromatography and potentiometry with selective electrode were used for the determination of nickel, sulfate and ammonium respectively.

3. Results and discussion

3.1.Control charts and reproducibility of images

As image control method, Shewhart control charts were made from the color standard [21]. These control charts let us know if an obtained image is suitable for image analysis or not. Additional information of these control method is included in the Supplementary Material.

3.2.Interpretation of image data

The first step was to relate some of the channels of RGB color space with the concentration of each analyte. For this, instead of the value of the intensity of color value of a channel, the expression $\log I_0/I$ was used [22] where I means the color intensity of each well in the chosen channel and I_0 is the intensity of the blank, being a well filled with double distilled water.

As regards to nickel, the channel that shows the best correlation with the concentration is the R channel of the RGB color space, since red is complementary to the green color of the solution. For ammonium, a good correlation was found with the B channel and analyte concentration, in this case because blue color is complementary to orange.

Instead, the concentration of sulfate showed no correlation with any of the channels of RGB color space, because in this case a white precipitate is used for quantitation of sulfate. Instead, the S channel of the HSV color space was found to correlate with the sulfate concentration, since it explains the transition of white to any color. In order to improve this transition, a red cardboard was placed on the metal cover of the scanner (see figure S2 in Supplementary Material). Due to the use of a different background, the intensity of the colors of the color pattern also varies, therefore, new control charts must be generated under these conditions.

3.3. Validation of methods

For the validation of the developed methods by image analysis, firstly the limit of detection (LOD) was calculated by multiplying 3.3 times the typical error of the regression ($s_{y/x}$) divided with the slope of the corresponding regression line. Results are shown in table 1. For nickel, sulfate and ammonium LODs are 0.5 g L^{-1}, 0.05 g L^{-1} and $5 \cdot 10^{-4}$ g L^{-1} respectively and linear ranges go from 1.0 to 10.0 g L^{-1} for nickel, 0.1 to 0.7 g L^{-1} for sulfate and from $1.0 \cdot 10^{-3}$ to $5.0 \cdot 10^{-3}$ g L^{-1} for ammonium. In all three cases, very good regressions were obtained, with R^2 values above 0.99.

To evaluate the precision, the repeatability and reproducibility values were calculated by the relative standard deviations (RSD %). The repeatability was measured at two levels of concentration with nine replicates of each and all measured in the same image. For reproducibility, two levels and nine replicates were also used, but this time three images taken on different days were used. Results are shown in table 1.

Table 1. Analytical figure of merits for nickel, sulfate and ammonium determinations by DIA.

Analyte	**Lineal range (g L^{-1})**	**R^2**	**LOD (g L^{-1})**	**Concentration level (g L^{-1})**	**Repeatability (RSD %, n=9)**	**Reproducibility (RSD %, n=9)**
Nickel	2.0 - 10.0	0.997	0.5	4.0	7.3	8.6
				9.0	4.2	3.8
Sulfate	0.10 - 0.70	0.995	0.05	0.30	8.4	12
				0.6	8.3	7.4
Ammonium	$(1.0 – 5.0) \cdot 10^{-3}$	0.994	$5 \cdot 10^{-4}$	$1.0 \cdot 10^{-3}$	12	14
				$4.0 \cdot 10^{-3}$	7.4	9.6

Taking into account the simplicity of the methods and instruments used, the RSD values shown in the table are satisfactory, since they are around 10% in all cases. For repeatability, only the lowest concentration for ammonium exceeds that limit of 10%, while for reproducibility, and considering different images, only two of the solutions are above 10%. Especially good results were obtained for nickel, since this component is not depending on any reaction to give a colored solution. It shows better precision than sulfate or ammonium.

3.4.Application to real samples

The above-described DIA procedure was applied to the determination of nickel, sulfate and ammonium in 10 samples from an electroless nickel bath and 3 samples from an electrolytic nickel bath. In order to evaluate the results obtained by DIA, the samples were also analyzed by the reference techniques described in the experimental section. The obtained results are shown in Table 2.

Table 2. Predicted concentrations in real sample for the three analytes. Average values of replicate samples (n=3) with standard deviations are shown. Letters indicate: Q = bath sample of electroless nickel, B = bath sample before nickel feedback A = bath sample after nickel feedback, E = sample of nickel electrolytic bath; DIA =Digital Image Analysis; UV-Vis = UV-Vis spectrometry, IC = Ionic Chromatography, Pot. = Potentiometry

	Nickel (g L^{-1})		**Sulfate (g L^{-1})**		**Ammonium (g L^{-1})**	
Sample	**DIA**	**UV-Vis**	**DIA**	**IC**	**DIA**	**Pot.**
Q5 - B	6.5 ± 0.2	6.4*	9.5 ± 0.2	10.33 ± 0.01	10.7 ± 0.4	10.7*
Q5 - A	8.2 ± 0.3	7.7*	12.3 ± 1.8	11.48 ± 0.05	11.6 ± 1.7	11.2*
Q10 - A	8.3 ± 0.6	7.6*	13.9 ± 0.1	14.88 ± 0.02	16.1 ± 0.4	16.3*
Q15 - B	7.3 ± 0.5	6.3*	20.9 ± 0.5	22.80 ± 0.04	25.1 ± 1.7	34.9*
Q15 - A	8.5 ± 1.1	7.0*	26 ± 3	27.70 ± 0.02	31 ± 3	22.7*
Q19 - B	7.8 ± 0.9	6.2*	28.6 ± 0.7	31.80 ± 0.01	37 ± 4	30.5*
Q19 - A	8.3 ± 0.2	8.2*	29.7 ± 0.6	32.05 ± 0.06	37 ± 6	31.2*
Q24 - A	9.8 ± 0.4	8.8*	39.5 ± 1.5	45.5 ± 0.7	47 ± 2	42.7*
Q28 - B	7.9 ± 0.8	8.4*	42.1 ± 1.8	46.6 ± 0.2	51 ± 3	45.5*
Q28 - A	8.0 ± 1.0	8.8*	45.6 ± 0.4	48.0 ± 0.3	51 ± 7	46.1*
E1	66 ± 3	67.4 ± 0.4	106.3 ± 0.4	106 ± 7	-	-
E2	67 ± 4	66.2 ± 1.7	100 ± 5	95.0 ± 1.04	-	-
E3	66.7 ± 1.7	67.4 ± 0.9	97 ± 9	103.8 ± 1.8	-	-

* Replicates were not performed due to insufficient volume of sample.

The obtained results follow the expected trend. On one hand, nickel concentration increases each time this metal is added in electroless nickel bath samples (identified with the letter A). In addition, the concentrations of sulfate and ammonium increase progressively as the bath is running. These compounds are also added when bath is fed with nickel. On the other

hand, the concentration of the analytes in the electrolytic nickel bath remains roughly constant because in this case no feedback has been made between samples.

To check if there are significant differences between the methods used for nickel determination, DIA and UV-Vis spectrophotometry, a *t-test* for paired samples was performed. For a total of 13 samples and for a confidence interval of 95%, no significant differences were found. Therefore, nickel can be equally determined by either DIA or UV-Vis spectrophotometry.

For the other two analytes, ammonium and sulfate, and due to the great span of the concentrations calculated for the samples, the representation of the found concentration *vs* added concentration has been performed to check for significant differences between methods.

In order to check if there are systematic errors, regarding the reference values extracted from the reference method, a joint confidence ellipse test for slope and intercept was accomplished. Mathematics and applications of the test has been given in bibliography [23,24]. A systematic

error produces a change in the slope from unity and a change in the intercept from zero.

Under these conditions, a slope of 1.00 ± 0.06 and a y-intercept of -2.04 ± 3.34 was obtained for sulfate. The ideal values are within these confidence intervals, which means that there are no significant differences between the methods. For ammonium, a value of 1.09 ± 0.0.30 was obtained for the slope and a value of -0.060 ± 9.61 for the y-intercept. Again, the ideal values lie within these confidence intervals. Fig. S3 in Supplementary Material shows the 95% confidence region for the true slope (1) and intercept (0). As it can be seen, this point falls within the ellipse, which means that no significant difference has been proven between reference methods and the developed method with DIA.

As mentioned before, real samples were also used to evaluate the accuracy of the method through recovery tests. In the case of nickel, 2.5 and 5.0 g L^{-1} of nickel were added to each sample, level 1 (L1) and level 2 (L2) respectively. For sulfate, levels L1 and L2 were obtained

adding 0.125 and 0.250 g L^{-1}. Finally, for ammonium, $1.08 \cdot 10^{-3}$ and $2.16 \cdot 10^{-3}$ g L^{-1} were added for levels L1 and L2 respectively. Table 3 shows the recovery (%) values obtained in each case.

As can be seen in Table 3, recovery values are in the range of 90 - 110%, with some exceptions. From this, it can be deduced that the matrix of the samples does not interfere with the determination of the analytes and that the accuracy of the methods is acceptable. As it has seen before, the best results were obtained for nickel.

Table 3. Main recovery percentages (%) for the three components: nickel, sulfate and ammonium in real samples. Each compound was spiked up to two different levels, level 1 (L1) and level 2 (L2). Average values of replicate samples (n=3) are shown with their standard deviations. In the case of electroless nickel bath samples, the volume provided was not enough for replicates.

Samples	Nickel (%)		Sulfate (%)		Ammonium (%)	
	L1	L2	L1	L2	L1	L2
Q5 – B	100	101	98 ± 9	102 ± 13	106 ± 6	102 ± 6
Q5 – A	94	93	88 ± 11	89 ± 10	99 ± 8	96 ± 7
Q10 – A	115	108	82 ± 12	95 ± 8	95 ± 3	90 ± 7
E1	104 ± 9	103 ± 7	105 ± 4	108 ± 7	-	-
E2	106 ± 9	111 ± 3	87 ± 7	88 ± 5	-	-
E3	106 ± 13	110 ± 18	82 ± 15	103 ± 2	-	-

3.5 Comparison of the developed method with other works

The obtained figures of merit of the method were compared with other works for the three analytes (Table 4). As it can be seen, nickel has been determined in different kind of samples. Linear ranges and accordingly the LOD values are lower in other applications (water, soil and chocolate analysis) [25], but is worth remarking that in this work the linear range was adjusted to working conditions and nickel is much more concentrated in nickel baths than in the other samples. A similar linear range has been used with SIA-spectrophotometry for nickel bath samples as well [26].

Sulfates have been determined with SIA-spectrophotometry [27] and X-ray fluorescence after a precipitation procedure [28] in several samples. Again, the linear ranges and consequently the

LOD values are lower but similar recovery values are obtained after application to samples, but both spectrophotometry and X-ray fluorescence are robust and well-known methods.

In the case of ammonium, image analysis has also been applied in wastewaters [29] and in this case our method it the one that shows lower linear range and LOD. On the other hand, when potentiometry is used [30], better results are obtained, as expected, considering that the analyzed samples (water and soils) are less complex than the ones used in the presented method.

The main advantages of DIA methodology are that it does not require a sophisticated equipment and the cost of analysis is much cheaper than in other procedures. Moreover, it is worth mentioning that the application of the presented method is focused on electrolytic and electroless nickel baths, and thus, parameters, such as the linear ranges, were adjusted to the requirements of the samples.

Table 4. Comparison table of analytical figure of merits for nickel, sulfate and ammonium determinations.

Analyte	**Method**	**Samples**	**Lineal range (g L^{-1})**	**R^2**	**LOD (g L^{-1})**	**RSD %**	**Recovery (%)**	**Ref.**
Nickel	DIA	Electroless nickel bath, electrolytic nickel bath	2.0 - 10.0	0.997	0.5	3.8-8.6	93-115	This work
Sulfate	DIA	Electroless nickel bath, electrolytic nickel bath	0.10 - 0.70	0.995	0.05	7.4-12	82-108	This work
Ammonium	DIA	Electroless nickel bath	$1.0\cdot10^{-3}$ – $5.0\cdot10^{-3}$	0.994	$5\cdot10^{-4}$	7.4-14	95-106	This work
Nickel	Spectrophotometry	River water, soils, chocolate, spring water	$0.1\cdot10^{-3}$-$25\cdot10^{-3}$	0.9989	$0.12\cdot10^{-6}$	1.3	99-102	[23]
Nickel	SIA-Spectrophotometry	Nickel electroplating bath	6 - 94	0.9981	-	0.2-3.3	-	[24]
Sulfate	SIA-MCR	Water, biodiesel	$0\cdot10^{-3}$-$15\cdot10^{-3}$	0.9902	$1.42\cdot10^{-3}$	-	85.5-123.5	[25]
Sulfate	X-ray fluorescence after a precipitation procedure	Ethanol fuel	$5.0\cdot10^{-5}$ – $2.0\cdot10^{-3}$	0.998	$3.0\cdot10^{-5}$	5.9	-	[26]

Ammonium	DIA	Wastewater	$10 \cdot 10^{-3}$-$100 \cdot 10^{-3}$	0.9889	$4 \cdot 10^{-3}$	-	-	[27]
Ammonium	Potentiometry	Environmental samples (water, soil)	$9 \cdot 10^{-5}$-0.018	0.98	$2.16 \cdot 10^{-5}$	-	-	[28]

4. Conclusions

It has been proven that image analysis is an effective technique to determine several analytes of a nickel bath by relating the concentration of these compounds to a color channel that can be extracted from an image of the bath. In this case, a desktop scanner has been used as an image capture device and good regressions as well as good analytical parameters have been obtained. In addition, no significant differences were found in the determination of nickel, sulfate and ammonium by image analysis, compared to different reference techniques, when these compounds are determined in real nickel bath samples. The reference techniques are probably more robust, and of greater precision and accuracy than the method proposed here, but image analysis offers certain advantages. These include the low cost of the instrumentation, the low consumption of reagents and samples volume (a maximum of 400 μL is used) and the possibility of analyzing several samples at the same time in a single image, which involves lot of time-saving. Finally, it is also worth mentioning that the taking of images has shown to be reproducible, and that this can be controlled by the use of a color chart in the image.

Acknowledgments

The authors acknowledge financial support from Diputación Foral de Gipuzkoa (Project DG 17/07) and University of the Basque Country (Projects GIU 16/55 and US 18/09). Authors are also grateful to Cidetec-Surface Engineering (Donostia, Spain) for supplying electroless nickel bath samples.

References

[1] N. Kanani, Electroplating: Basic principles, processes and practice. (2004). Elsevier.

[2] G. O. Mallory, and J. B. Hajdu, Electroless plating: Fundamentals and applications. (1990). William Andrew.

[3] J. Wojciechowski, M. Baraniak, J. Pernak, and G. Lota, Nickel Coatings Electrodeposited from Watts Type Baths Containing Quaternary Ammonium Sulphate Salts Int. J. Electrochem. Sc., 12 (2017) 3350-3360. https://doi.org/10.20964/2017.04.70

[4] E. K. Baran, and S. B. Yaşar, Zinc and nickel determination in liquid edible oils by FAAS after the extraction Eur. J. Lipid Sci. Tech., 114 (2012) 1320-1326. https://doi.org/10.1002/ejlt.201100081

[5] S. L. Ferreira, C. F. de Brito, A. F. Dantas, de Araujo, Neyla M Lopo, and A. S. Costa, Nickel determination in saline matrices by ICP-AES after sorption on Amberlite XAD-2 loaded with PAN Talanta, 48 (1999) 1173-1177. https://doi.org/10.1016/S0039-9140(98)00339-7

[6] M. Ostra, C. Ubide, M. Vidal, and J. Zuriarrain, Process analytical chemistry in a nickel electroplating bath. Automated sequential injection for additive determination Anal. Methods, 3 (2011) 2726-2732. https://doi.org/10.1039/C1AY05434A

[7] C. Bosch Ojeda, F. Sánchez Rojas, and J. Cano Pavón, A greener and sensitive procedure for nickel determination by cloud point extraction and UV/Vis spectrophotometry Res. J. Pharm. Biol. Chem. Sci., 1 (2010) 514-523.

[8] P. Licata, F. Naccari, G. Di Bella, V. Lo Turco, V. Martorana, and G. mo Dugo, Inorganic anions in goat and ovine milk from Calabria (Italy) by suppressed ion chromatography Food Addit. Contam. A, 30 (2013) 458-465. https://doi.org/10.1080/19440049.2012.747222

[9] O. Zamora Martínez, J. M. Montaño Hilario, V. B. Galindo Zavala, C. Siebe Grabach, and B. L. Prado Pano, Determinación simultánea de cationes mayoritarios en muestras de agua residual por medio de cromatografía de iones con detección conductimétrica Rev. Int. Contam. Ambient, 32 (2016) 293-301.

[10] BOE, Boletín Oficial del Estado, Métodos oficiales de análisis físico-químicos para aguas potables de consumo público: Tomo I. (1998). Ministerio de agricultura, pesca y alimentación. Madrid.

[11] B. G. Botelho, K. C. F. Dantas, and M. M. Sena, Determination of allura red dye in hard candies by using digital images obtained with a mobile phone and N-PLS Chemometrics and Intelligent Laboratory Systems, 167 (2017) 44-49. https://doi.org/10.1016/j.chemolab.2017.05.004

[12] A. Antonelli, M. Cocchi, P. Fava, G. Foca, G. C. Franchini, D. Manzini, and A. Ulrici, Automated evaluation of food colour by means of multivariate image analysis coupled to a wavelet-based classification algorithm Anal. Chim. Acta, 515 (2004) 3-13. https://doi.org/10.1016/j.aca.2004.01.005

[13] B. G. Botelho, L. P. de Assis, and M. M. Sena, Development and analytical validation of a simple multivariate calibration method using digital scanner images for sunset yellow determination in soft beverages Food Chem., 159 (2014) 175-180. https://doi.org/10.1016/j.foodchem.2014.03.048

[14] M. Vidal, R. Garcia-Arrona, A. Bordagaray, M. Ostra, and G. Albizu, Simultaneous determination of color additives tartrazine and allura red in food products by digital image analysis Talanta, 184 (2018) 58-64. https://doi.org/10.1016/j.talanta.2018.02.111

[15] M. Saraji, and N. Bagheri, Paper-based headspace extraction combined with digital image analysis for trace determination of cyanide in water samples Sensor Actuat B-Chem., 270 (2018) 28-34. https://doi.org/10.1016/j.snb.2018.05.021

[16] M. Vidal, M. Ostra, N. Imaz, E. García-Lecina, and C. Ubide, Feature descriptors from scanned images of chromium electrodeposits as predictor parameters of surface roughness and crystallographic texture Chemometr. Intell. Lab., 149 (2015) 90-98. https://doi.org/10.1016/j.chemolab.2015.10.004

[17] M. Vidal, J. M. Amigo, R. Bro, M. Ostra, C. Ubide, and J. Zuriarrain, Flatbed scanners as a source of imaging. Brightness assessment and additives determination in a nickel electroplating bath Anal. Chim. Acta, 694 (2011) 38-45. https://doi.org/10.1016/j.aca.2011.03.030

[18] M. Vidal, J. M. Amigo, R. Bro, Van Den Berg, Frans WJ, M. Ostra, and C. Ubide, Image analysis for maintenance of coating quality in nickel electroplating baths–Real time control Anal. Chim. Acta, 706 (2011) 1-7. https://doi.org/10.1016/j.aca.2011.08.007

[19] L. F. Capitan-Vallvey, N. Lopez-Ruiz, A. Martinez-Olmos, M. M. Erenas, and A. J. Palma, Recent developments in computer vision-based analytical chemistry: A tutorial review Anal. Chim. Acta, 899 (2015) 23-56. https://doi.org/10.1016/j.aca.2015.10.009

[20] M. Vidal, J. M. Amigo, R. Bro, M. Ostra, and C. Ubide, Quantitative determination of additives in a commercial electroplating nickel bath by spectrophotometry and multivariate analysis Anal. Methods, 2 (2010) 86-92. https://doi.org/10.1039/B9AY00158A

[21] M. Vidal Postigo, New Methods for the Analytical Control of a Nickel Electroplating Bath. Application of Chemometric Techniques, (2010)

[22] S. K. Kohl, J. D. Landmark, and D. F. Stickle, Demonstration of absorbance using digital color image analysis and colored solutions J. Chem. Educ., 83 (2006) 644. https://doi.org/10.1021/ed083p644

[23] A. G. González, M. A. Herrador, and A. G. Asuero, Intra-laboratory testing of method accuracy from recovery assays Talanta, 48 (1999) 729-736. https://doi.org/10.1016/S0039-9140(98)00271-9

[24] H. C. Goicoechea, and A. C. Olivieri, Sustained prediction ability of net analyte preprocessing methods using reduced calibration sets. Theoretical and experimental study involving the spectrophotometric analysis of multicomponent mixtures Analyst, 126 (2001) 1105-1112. https://doi.org/10.1039/B100422K

[25] M. Ghaedi, Selective and sensitized spectrophotometric determination of trace amounts of Ni(II) ion using α-benzyl dioxime in surfactant media Spectrochimica Acta Part A: Molecular and Biomolecular Spectroscopy, 66 (2007) 295-301. https://doi.org/10.1016/j.saa.2006.02.055

[26] J. Edson da Silva, M. F. Pimentel, V. Lins da Silva, M. d. C. B. S. M. Montenegro, and A. N. Araújo, Simultaneous determination of pH, chloride and nickel in electroplating baths using sequential injection analysis Analytica Chimica Acta, 506 (2004) 197-202. https://doi.org/10.1016/j.aca.2003.11.016

[27] V. del Río, M. Soledad Larrechi, and M. Pilar Callao, Determination of sulphate in water and biodiesel samples by a sequential injection analysis—Multivariate curve resolution method Analytica Chimica Acta, 676 (2010) 28-33. https://doi.org/10.1016/j.aca.2010.07.028

[28] L. S. G. Teixeira, T. J. Chaves, P. R. B. Guimarães, L. A. M. Pontes, and J. S. R. Teixeira, Indirect determination of chloride and sulfate ions in ethanol fuel by X-ray fluorescence after a precipitation procedure Analytica Chimica Acta, 640 (2009) 29-32. https://doi.org/10.1016/j.aca.2009.03.032

[29] P. Jaikang, P. Paengnakorn, and K. Grudpan, Simple colorimetric ammonium assay employing well microplate with gas pervaporation and diffusion for natural indicator immobilized paper sensor via smartphone detection Microchemical Journal, 152 (2020) 104283. https://doi.org/10.1016/j.microc.2019.104283

[30] J. Choosang, A. Numnuam, P. Thavarungkul, P. Kanatharana, T. Radu, S. Ullah, and A. Radu, Simultaneous detection of ammonium and nitrate in environmental samples using on ion-selective electrode and comparison with portable colorimetric assays Sensors, 18 (2018) 3555. https://doi.org/10.3390/s18103555